High performance films of cellulose butyral derivative having a necklace-like annular structure in the side chains

AUTHOR(S):

Chang, Chunyu; Teramoto, Yoshikuni; Nishio, Yoshiyuki

High performance films of cellulose butyral derivative having a necklace-like annular structure in the side chains

Chunyu Chang[a,b], Yoshikuni Teramoto[a], Yoshiyuki Nishio[a*]

[a]*Division of Forest and Biomaterials Science, Graduate School of Agriculture, Kyoto University, Sakyo-ku, Kyoto 606-8502, Japan*

[b] *Guangzhou Sugarcane Industry Research Institute, Guangzhou 510316, China*

* To whom correspondence should be addressed. Tel: +81-757536250;

Email: ynishio@kais.kyoto-u.ac.jp (Prof. Y. Nishio).

ABSTRACT

We fabricated high performance films using cellulose butyral (CB) synthesized from native cellulose. Two-step reactions were adopted to produce the derivative CB, including etherification of cellulose with glycidol in NaOH/urea aqueous solution to yield *O*-(2,3-dihydroxypropyl) cellulose (DHPC), and butyralization of DHPC. Both DHPC and CB products were easily processed into a thin film by hot-press molding. The butyral modifier significantly improved the tenacity of highly ductile DHPC, by virtue of the possible chain-entangling action of the ring structures in the stretching process. Thereby the film toughness was markedly enhanced. The CB films exhibited excellent optical transparency and a good adhesive property to glass plates. Thus the films may be comparable to commercial poly(vinyl butyral) (PVB) films in optical and mechanical performances and therefore possess a potential applicability as interlayer for laminated glasses.

Keywords: *O*-(2,3-dihydroxypropyl) cellulose, Cellulose butyral, Interlayer of laminated glass.

1. Introduction

Poly(vinyl butyral) (PVB) is used in bulk as interlayer of laminated glasses, since the film can well adhere to glass surfaces and render an excellent mechanical resistance to the break of the laminate [1]. PVB is synthesized by reacting poly(vinyl alcohol) (PVA) with butyraldehyde (BuA) in an acidic medium. 1,3-Dioxane rings are formed in the acetalization, which probably contributes to the impact-resistance and toughness of PVB films. The residual hydroxyl groups on the PVB main skeleton should conduce to the adhesive property of the film products for safety glass interlayers, etc. Under the inspiration to the PVA-based commodity, we wondered if it is possible to create such interlayers from an inexhaustible natural resource, cellulose. Currently, much attention and great interest have been directed to the conversion of cellulose to advanced materials in connection with green and sustainable development of industry [2-6].

As regards mechanical properties of cellulosics, the tensile strength of regenerated cellulose films are mostly in a level of several tens of MPa and cellulose nanofiber-based films exhibit a strength of as high as hundreds of MPa, but their ultimate strains are lower than 10 % [7-9]. The high-stiff nature can not meet the requirement of rather ductile performance for interlayer of laminated glasses. Chemical modifications, blending, and hybridization of cellulose with other compounds or polymers can be effective methods to alter the mechanical properties of cellulose films [4, 10-12]. However, the "ductility" and "toughness" of cellulose-based films seem to be incompatible [13, 14]. Therefore, the challenge toward the development of impact-resistant interlayers from cellulose may be parallel to improving both the ductility and toughness of the film, desirably without any additive or filler. In addition, the high standards of the interlayer materials would require, in film form, optical transparency, a refractive index comparable to or rather lower than that (~1.51) of conventional glass, and adhesive property.

In our preceding work, we designed a pathway to synthesize novel cellulose

derivatives having a necklace-like structure in the side chains [15]. First, native cellulose was modified with glycidol (GLY) in NaOH/urea aqueous solution to obtain *O*-(2,3-dihydroxypropyl) cellulose (DHPC) having more than two hydroxyl groups in the side chains. Then, butyralization of DHPC with BuA was conducted in acidic aqueous solution, so as to produce cellulose butyral (CB) involving a cyclic acetal formation in the side chains. The objective of the present paper is to evaluate films of CB for the applicability as interlayer of laminated glasses. The CB materials were prepared through rigorous analysis of the molecular structure including the type of ring formation as well as the substituent contents.

2. Experimental

2.1 Synthesis of Cellulose Derivatives and Preparation of Films

The cellulose material used was a cotton linter pulp with an average degree of polymerization of 560. *O*-(2,3-dihydroxypropyl) cellulose (DHPC) was synthesized from the cotton cellulose and four products $DHPC_a$–$DHPC_d$ (**Table 1**) were characterized, according to the previous respective methods [15]. How to determine the structural parameters such as degree of substitution (DS) and secondary molar substitution (MS) will be discussed later. To improve the solubility of the DHPCs in common solvents and the resolution of their NMR spectra, thorough propionylation [16] of them was adopted as we had done previously [15]. Cellulose butyral (CB) samples were prepared by butyralization of DHPC with butyraldehyde (BuA) in a similar way to that described previously [15], but the reaction conditions were diversified (**Table 2**): 0.2–0.8 g of DHPC was dissolved into water to form a ~20 mL solution, in which *p*-toluene sulfonic acid (PTSA) (0.1 g) or 35 % HCl aq. (0.05 g) was also fed as a catalyst for dehydration. 6 to 50-eq BuA per OH group of DHPC was added dropwise into the solution, which was continuously stirred at a regulated temperature (50–90 ^{o}C) under a nitrogen atmosphere. After 10–96 h, the reaction mixture was neutralized with 0.1 M Na_2CO_3 solution, and then dialyzed against distilled water for 1 week. The purified solution was finally freeze-dried with a

lyophilizer to obtain the objective product CB, and coded as CB_a1 (from $DHPC_a$) or CB_b6 (from $DHPC_b$), etc.

Table 1. Results of DHPC synthesis from cotton cellulose in NaOH/urea aqueous solution at 25 °C.

Code	GLY/ AGU[a]	Time h	Total DS	DS at positions C2	C3	C6	MS_{dhp}	M_w[b] 10^4	M_n[b] 10^4	M_w/M_n[b]	DP_w
$DHPC_a$	96	48	1.76	0.57	0.38	0.81	9.16	33.4	12.3	2.7	213
$DHPC_b$	84	48	1.55	0.67	0.13	0.64	8.03	28.7	9.9	2.9	202
$DHPC_c$	72	36	1.51	0.53	0.38	0.60	6.43	28.5	9.8	2.9	237
$DHPC_d$	48	24	1.09	0.45	0.19	0.45	2.92	22.7	6.8	3.3	309

[a] Molar ratio of in-feed GLY to anhydroglucose unit (AGU); [b] Determined for propionylated DHPC (pDHPC) samples by GPC using THF as eluent.

Table 2. Reaction conditions[a] and product yield in the synthesis of CB from DHPC.

Code	DHPC g	BuA eq/OH	Catalyst[b]	Temperature °C	Time h	Yield g
CB_a1	$DHPC_a$, 0.2	25	PTSA	70	20	0.18
CB_a2	$DHPC_a$, 0.2	25	PTSA	80	20	0.14
CB_a3	$DHPC_a$, 0.2	25	PTSA	90	10	0.18
CB_a4	$DHPC_a$, 0.2	24	HCl	50	20	0.21
CB_a5	$DHPC_a$, 0.4	50	PTSA	90	20	0.27
CB_b6	$DHPC_b$, 0.8	24	HCl	50	20	0.75

CB_b7	$DHPC_b$, 0.8	48	HCl	50	60	0.79
CB_c8	$DHPC_c$, 0.4	6	HCl	50	25	0.41
CB_c9	$DHPC_c$, 0.4	24	HCl	50	25	0.37
CB_d10	$DHPC_d$, 0.4	11	HCl	50	50	0.36
CB_d11	$DHPC_d$, 0.4	22	HCl	50	96	0.36

[a] Solvent, ~ 20 mL distilled water.

[b] HCl, 0.05 g of 35 % hydrochloride acid; PTSA, 0.1 g of *p*-toluenesulfonic acid monohydrate.

CB films were prepared by hot-press molding with a pressing apparatus SA-302 (Tester Sangyo Ltd., Japan). CB powder was placed between two polished stainless-steel plates (20 × 20 cm^2), which were wrapped with PET films. Then, the CB was molded into a thin film at 130 °C under 20 MPa for 5 min, followed by quick cooling to 18 °C. The thickness was controlled to be 0.10 mm by using a metal spacer.

2.2 Characterizations of Cellulose Derivatives and Films

NMR measurements were carried out on a Varian NMR system 500 MHz with an OneNMR 5MM Probe. ^{13}C NMR spectra of cellulose derivatives were measured in the following conditions: solvent, dimethyl sulfoxide (DMSO)-d_6 or pyridine-d_5; temperature, 23 °C; solute concentration, 15 mg mL^{-1}; internal standard, tetramethylsilane (TMS); recycling time, 2 s; scan number, 20480. As regards ^1H NMR, the conditions of spectra measurements were as follows: solvent, $CDCl_3$; temperature, 23 °C; solute concentration, 10 mg mL^{-1}; scan number, 16. Molecular weight determination was performed by GPC with a Tosoh HLC-8220 GPC apparatus, in the following conditions: column, two Tosoh TSK Super HZM-H columns connected with each other; flow rate, 0.25 mg min^{-1}; temperature, 40 °C; eluent, tetrahydrofuran (THF); standard, monodispersed polystyrene.

UV-visible light absorption spectra of CB films were recorded on a U-4100 spectrophotometer (Hitachi, Japan). The transmittance of the films 0.10 mm thick was measured from 300 to 800 nm at a scanning rate of 60 nm min^{-1}. Refractive index was also measured for the CB films by using an Abbé refractometer (Atago 2T, Japan).

Differential scanning calorimetry (DSC) was carried out with a Seiko DSC6200/EXSTAR6000 apparatus calibrated with an indium standard. The measurements were made on ca. 4 mg samples each packed in an aluminum pan. First, the sample was heated from room temperature (20 °C) to 200 °C at a rate of 20 °C min^{-1} under a nitrogen atmosphere. Subsequently, the temperature was decreased to −100 °C with liquid nitrogen, and then the second heating scan was run from −100 °C to 200 °C at a rate of 10 °C min^{-1}. The glass transition temperature (T_g) was estimated in the second heating scan, from the midpoint of a base-line shift in heat flow characteristic of the transition.

Dynamic mechanical analysis (DMA) was conducted by using a Seiko DMS6100/EXSTAR6000 apparatus in tension mode, usually at an oscillatory frequency (f) of 1 Hz. The temperature ranged from −150 to 200 °C, and the heating rate was 2 °C min^{-1}. The test specimen was a thin rectangular strip (20 mm × 5 mm × 0.1 mm) cut from a clear portion of the thermally molded films. To estimate an activation energy regarding major relaxation signals, various frequencies (f = 0.5, 1, 2, 5, and 10 Hz) were adopted. Similar rectangular strips cut from another portion of the films were subjected to a tensile mechanical test using a Shimazu Autograph AGS-5kNG. The measurements were done at 23 °C and 50 % r. h. with an elongation rate of 0.1 mm min^{-1}. Three strips obtained from a given larger film were tested and average values were adopted for the specific tensile data listed.

3. Results and Discussion

3.1 Structure determination of cellulose derivatives

Four samples of DHPC as precursor were obtained from cotton cellulose in various

conditions to provide different DS and MS values, where DS and MS are defined as an average number of the substituted hydroxyl groups and that of the substituent groups introduced in total, respectively, per anhydroglucose unit (AGU). **Fig. 1** illustrates a ^{13}C NMR spectrum (data a) of a DHPC product ($DHPC_d$ listed in **Table 1**). Sharp peaks derived from the carbons of dihydroxypropyl side-chains were all coded as C*. C1 and C1' signals were attributed to either of the two species of C-1 carbon in AGU of cellulose, according to whether the carbon C-1 adjoined unsubstituted C-2 or substituted C-2 in AGU (C1' as regards the latter case). C2 and C2' signals were also differentiated, according to whether the carbon C-2 was uninvolved or involved in the hydroxyl substitution (C2' as regards the latter case). In a similar way, the other signals were reasonably assigned to different carbons of DHPC [15]. By using the peak areas of C1, C1', and C6 as well as the overlapping peak area of C2' and C3', we can calculate DS for each DHPC sample by **Eq. (1)**:

$$DS = DS_{C2} + DS_{C3} + DS_{C6} = \frac{\mathbf{A}_{C1} + (\mathbf{A}_{C2} + \mathbf{A}_{C3} - \mathbf{A}_{C1'}) + (\mathbf{A}_{C1} + \mathbf{A}_{C1} - \mathbf{A}_{C6})}{\mathbf{A}_{C1} + \mathbf{A}_{C1'}} \quad (1)$$

where the three major terms in the fractional numerator refer to DS_{C2}, DS_{C3}, and DS_{C6} in turn, and $\mathbf{A}_{C1}$ and $\mathbf{A}_{C6}$ are the peak areas of C1 and C6 uninvolved in the hydroxyl substitution, while $\mathbf{A}_{C1'}$, $\mathbf{A}_{C2'}$, and $\mathbf{A}_{C3'}$ are the peak areas of C1', C2', and C3' participating in the substitution. In the above formulation, $\mathbf{A}_{C2'}$ and ($\mathbf{A}_{C6}$+$\mathbf{A}_{C6'}$) ($\mathbf{A}_{C6'}$, peak area of C6') are taken as being equivalent to $\mathbf{A}_{C1'}$ and ($\mathbf{A}_{C1}$+$\mathbf{A}_{C1'}$), respectively. **Fig. 1** also exemplifies a ^{1}H NMR spectrum (data b) of fully propionylated $DHPC_d$ ($pDHPC_d$). This full propionylation of DHPC was conducted to precisely quantify the molar dihydroxypropyl substitution MS_{dhp} [15]. In the ^{1}H spectrum, we can see a discrete peak of one proton (C-2H) in AGU (**A**) and intense signals coming from two protons of methylene group (**B**) and from three protons of methyl group (**C**) in the propionyl substituent. Therefore, MS_{dhp} of DHPC can be determined by using **Eq. (2)**:

$$MS_{dhp} = \frac{\mathbf{B}/2 - 3\mathbf{A}}{\mathbf{A}} = \frac{\mathbf{C}/3 - 3\mathbf{A}}{\mathbf{A}} \quad (2)$$

As a result of relevant analyses, the data of DS ranged from 1.09 ($DHPC_d$) through 1.51 ($DHPC_c$) and 1.55 ($DHPC_b$) to 1.76 ($DHPC_a$) and the value of MS_{dhp} varied as 2.92 ($DHPC_d$), 6.43 ($DHPC_c$), 8.03 ($DHPC_b$), and 9.16 ($DHPC_a$). All the DHPC

samples were water-soluble, and therefore distilled water was usable as a common solvent for their butyralization with BuA under various conditions **(Table 2**).

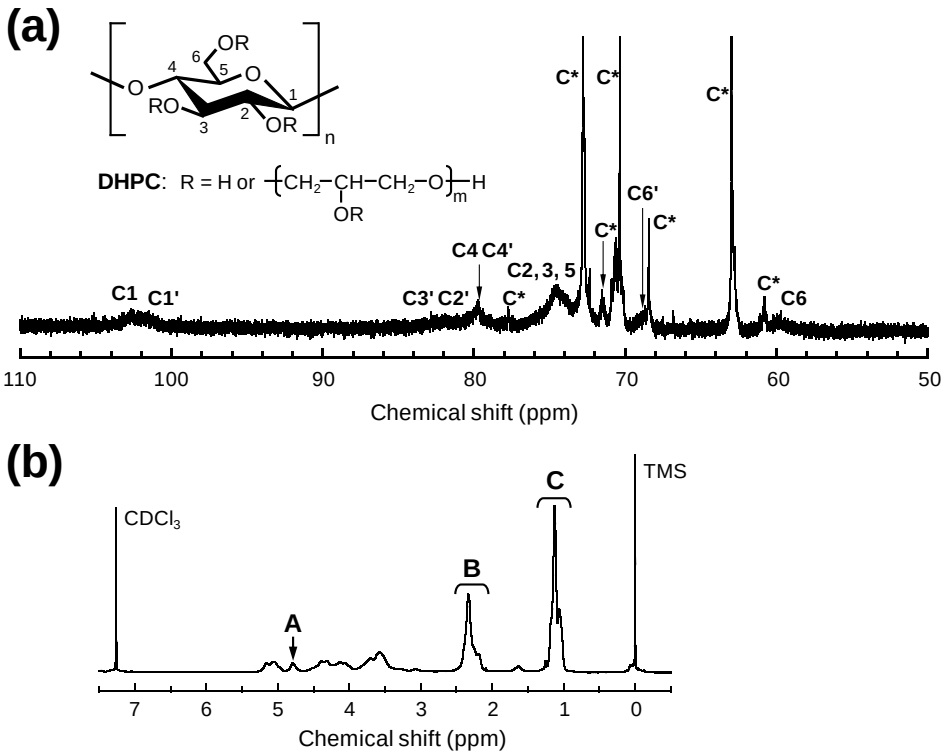

Fig. 1. Spectral examples: (a) ^{13}C NMR for DHPC in DMSO-d_6; (b) ^{1}H NMR for pDHPC in $CDCl_3$.

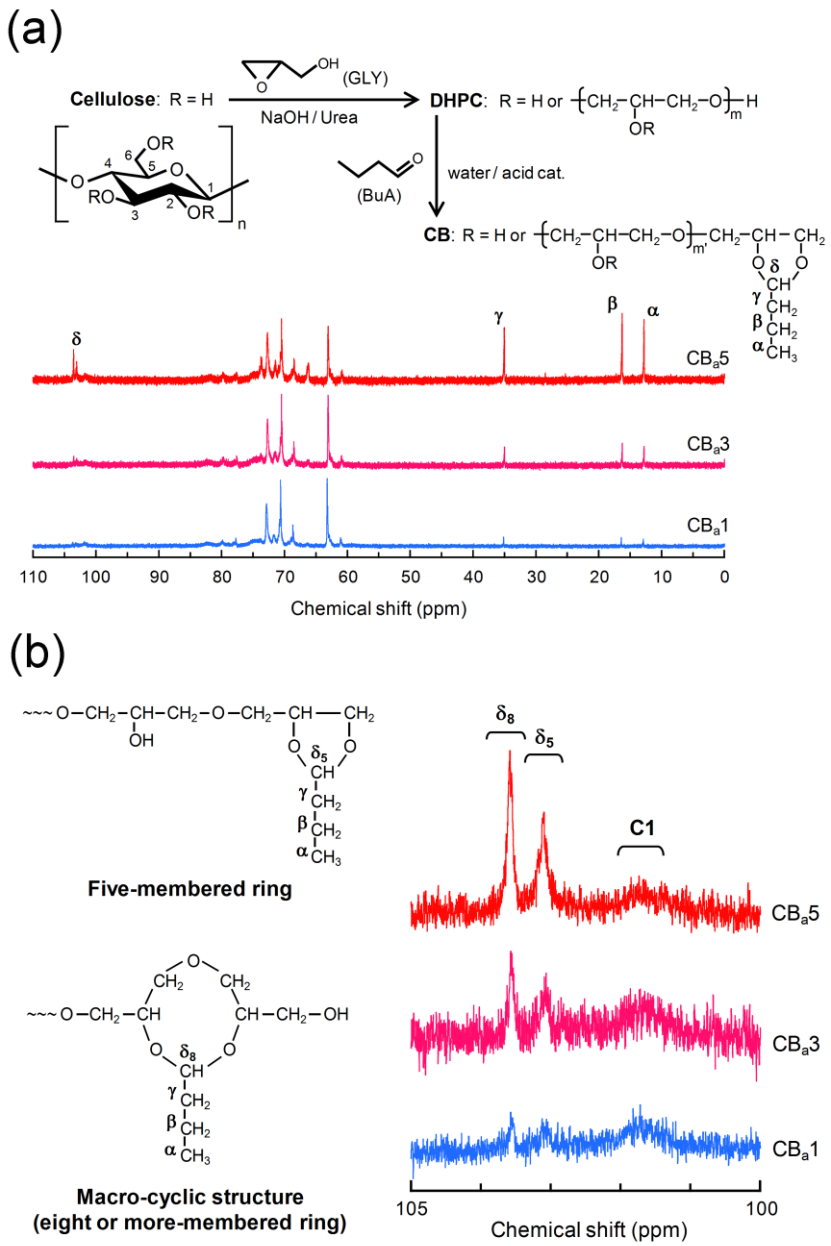

Fig. 2. (a) ^{13}C NMR spectra of CB products in pyridine-d_5 solution and the assignment for the butyral carbons, together with structural formulation of the derivatization; (b) enlarged ^{13}C NMR spectra in a range of 100–105 ppm and peak assignments.

Fig. 2a illustrates ^{13}C NMR spectra of CB$_a$1, CB$_a$3, and CB$_a$5 (all derived from DHPC$_a$) in pyridine-d_5. A peak of the methyl carbon (α) of introduced butyral groups appeared at 14.0 ppm. Two methylene carbon peaks from the group arose at 17.5 and 36.3 ppm, which are assigned as β and γ, respectively. Many signals appearing in a

range of 60–103 ppm were attributed to DHPC carbons (**Fig. 1a**). For plural peaks gathering in 101–105 ppm, the assignments are made clearer on enlarged spectra in **Fig. 2b**. A broad peak centered at ~101.5 ppm is associated with C1 of AGU, and two peaks situated at 103.7 ppm (δ_8) and 103.2 ppm (δ_5) are both coming from resonance of the butyral methine carbon (δ). This splitting of δ indicates that two kinds of annular structures were formed in the side chains of dihydroxypropyl sequence, following the butyralization of DHPC. One is a standard five-membered ring generated by reaction of BuA with the duplicate hydroxyls at the end of one side-chain. The other is a macro-cyclic structure (involving eight or more atoms) formed by butyralization with two hydroxyl groups belonging to mutually different dihydroxypropyl units. In the present study, the NMR peak-height ratio (δ_8/δ_5) was estimated, indexing a relative proportion of the eight and more-membered rings to the five-membered one. In this regard, CB products from DHPC of particularly high MS_{dhp}, just like CB_a from $DHPC_a$, would contain larger sizes of macro-cyclic structure such as eleven-membered and fourteen-membered rings, in addition to the octatomic ring.

By using the areas of the carbon peaks α, β, γ, and C1 assigned in ^{13}C NMR data (**Fig. 2**) for the CB products, we can estimate the MS of butyral groups ($MS_{butyral}$) at an average value from **Eq. (3)**:

$$MS_{butyral} = \frac{\mathbf{A}_{Cbutyral}}{\mathbf{A}_{C1}} = \frac{(\mathbf{A}_{\alpha} + \mathbf{A}_{\beta} + \mathbf{A}_{\gamma})/3}{\mathbf{A}_{C1}} \quad (3)$$

where $\mathbf{A}_{Cbutyral}$ represents an average value of the resonance peak areas of the butyral carbons α–γ, and $\mathbf{A}_{C1}$ is the peak area of C1. As additional structural parameters, the weight contents of dihydroxypropyl (% Dhp) and butyral moieties (% Butyral) and the remainder (% AGU) can be calculated from **Eqs. (4), (5),** and **(6)**, respectively:

$$\%\,Dhp = \frac{75MS_{dhp}}{162 - DS + 75MS_{dhp} + 56MS_{butyral}} \times 100 \quad (4)$$

$$\%\,Butyral = \frac{56MS_{butyral}}{162 - DS + 75MS_{dhp} + 56MS_{butyral}} \times 100 \quad (5)$$

$$\%\,AGU = 100 - \%Dhp - \%Butyral \quad (6)$$

where three numerals 162, 75, and 56 denotes the formula weights of AGU, dihydroxypropyl substituent, and butyl group, respectively.

The result of the CB productions is summarized in **Table 3**. Except for two products from $DHPC_d$ (CB_d10 and CB_d11, insoluble in pyridine), nine CBs were successfully synthesized from $DHPC_a$ (CB_a1–CB_a5), $DHPC_b$ (CB_b6 and CB_b7), and $DHPC_c$ (CB_c8 and CB_c9), offering values of % Butyral ranging from 1.0 to 19.2 % and of % Dhp varying from 65.5 to 80 %. CB_d10 and CB_d11 seem to have remained virtually non-butylarized $DHPC_d$ under the reaction conditions adopted, possibly due to its relatively low dihydroxypropyl substitution (DS = 1.09, MS_{dhp} = 2.92). The others CB_a1–CB_c9 were all soluble in pyridine and insoluble in water, as a result of the introduction of hydrophobic butyral groups. Surprisingly, this applied to even CB_a1 and CB_c8 of 1–1.5 % Butyral.

Table 3. Structure parameters of CB products, and thermal and mechanical properties of hot-pressed CB films.

Code	$MS_{butyral}$	δ_8/δ_5	% Butyral	% Dhp	% AGU	T_g °C	T_α °C	σ_b MPa	ε_b %	Toughness MPa
$DHPC_a$	0	–	0	81.1	18.9	20.3	25	0.99	267	2.0
CB_a1	0.20	1.1	1.3	80.0	18.7	17.8	–	1.95	209	2.6
CB_a2	0.75	1.6	4.7	77.2	18.1	16.2	–	3.33	164	4.2
CB_a3	0.94	1.3	5.8	76.4	17.8	–	−2	3.07	203	4.2
CB_a4	1.72	1.6	10.2	72.8	17.0	–	−7	2.41	213	4.3
CB_a5	3.60	1.7	19.2	65.5	15.3	14.1	−10	1.55	231	2.4
$DHPC_b$	0	–	0	79.0	21.0	20.6	25	1.71	196	2.0
CB_b6	0.54	1.3	3.8	76.0	20.2	18.2	20	7.51	151	8.7

CB_b7	1.16	1.5	7.8	72.7	19.5	18.0	12	13.3	81	6.0
$DHPC_c$	0	–	0	75.0	25.0	18.6	20	3.69	145	3.5
CB_c8	0.11	0.92	1.0	74.3	24.7	13.1	17	11.0	78	5.3
CB_c9	0.39	0.72	3.3	72.6	24.1	12.0	1	6.12	98	4.4
$DHPC_d$	0	–	0	57.6	42.4	–	–	–	–	–
CB_d10	–	–	–	~57	~43	–	–	–	–	–
CB_d11	–	–	–	~57	~43	–	–	–	–	–

T_g, from DSC; T_α, from DMA (E'' data); σ_b, tensile strength; ε_b, elongation at break.

3.2 Properties of cellulose butyral films

Visual appearance of a thermally molded film of CB_c8 (0.10 mm thick) is shown in **Fig. 3a**, exemplifying an excellent transparency. In **Fig. 3b**, light transmittance of the CB_c8 film is plotted against wavelength in a range of 300–800 nm, together with the corresponding data for a comparative film of $DHPC_c$. The transmittance of the respective samples rose rapidly with an increase of wavelength up to ~420 nm, and, above the wavelength of blue light, it gradually increased to reach 86.4 % as to CB_c8 and 83.2 % as to $DHPC_c$ at 800 nm of red light. The optical clarity of the CB_c8 film was quite stable against temperature variation in a practical range of −20–60 °C, where the transmittance remained constant at 84 % for a visible light of 550 nm. Refractive index (n) data, n = 1.496–1.501, were also estimated for films of CB_a and CB_c products by using an Abbé refractometer, but those of the corresponding DHPC precursors were somewhat higher (1.505–1.508). The n values for CBs are appreciably lower than that (n = 1.54) of cellulose, and this situation is similar to a relation between PVB (n = 1.48–1.49) and PVA (n = 1.51–1.53) [17]. Not only the film transparency against visible lights but also the refractive index being a little under that (n = ~1.51) of conventional glass, disclosed for CB, can meet the optical

demand for adoption as a polymer interlayer of laminated glasses.

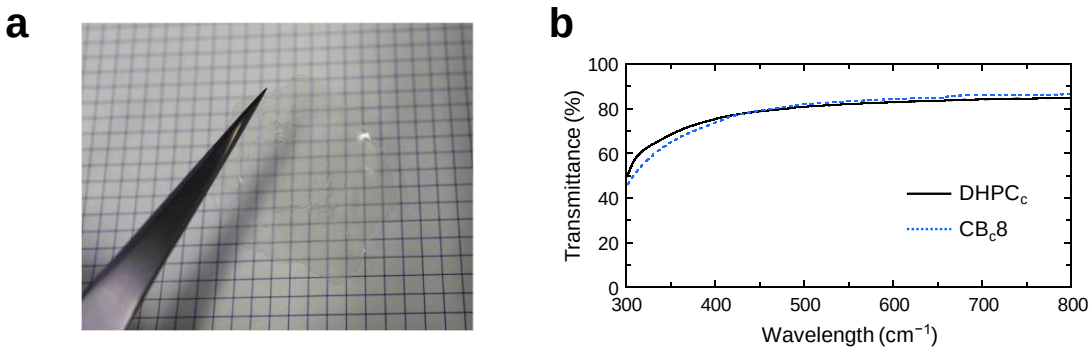

Fig. 3. (a) Visual appearance of hot-pressed CB_c8 film; (b) optical transparency of $DHPC_c$ and CB_c8 films under UV-Vis light (300–800 nm).

In DSC measurements, all the test samples of DHPC and CB exhibited only a T_g signal and gave no indication of crystal development (see **Fig. 4**). This non-crystalline uniformity should be responsible for the high clarity of the films. DHPCs gave a T_g value of 19–21 °C, and another lower T_g of 12–18 °C was observed for the derivative CBs (see data in **Table 3**). Such slight descent of T_g has also been experienced after butyralization of PVA (T_g = 70–85 °C) to produce PVB (T_g = 60–80 °C) [18]. In visual inspection, the CB films were rubbery or rather sticky at room temperature (~25 °C) and functioned as adhesive tape between slide glasses. Concerning thermal degradation of the CB derivatives, they signalized no decomposition at temperatures lower than ~240 °C in thermal gravimetric analysis (see Supplementary Information, **Fig. S1**).

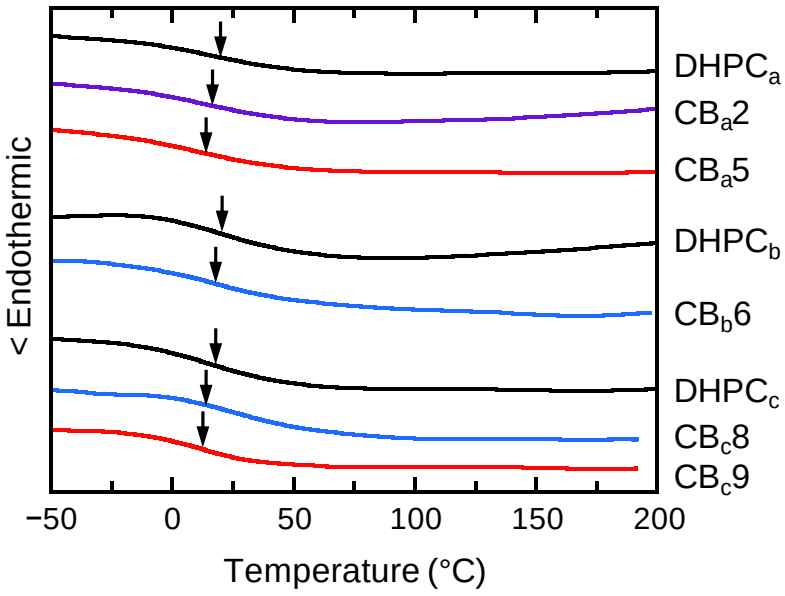

Fig. 4. DSC thermograms for selected films of DHPC and CB. Arrows indicate a T_g position taken as the midpoint of a baseline shift in heat flow.

Fig. 5a shows a DMA result for DHPC$_c$ and CB$_c$9 films, making a comparison of the temperature dependence of E', E'', and tanδ between the two. In the data set of the respective samples, we can find three distinctive dispersions, designated as β, α, and α_H from the lower temperature side. For DHPC$_c$, the β and α dispersions are observed at ca. −40 °C and 20 °C, respectively, as estimated from the corresponding E'' peaks. The α_H dispersion is, however, rather latent above 70 °C in the DHPC sample, when viewed from the E' and E'' data. After DHPC$_c$ was butyralized into CB$_c$, the former two dispersions shifted toward the lower temperature side, while the α_H dispersion became noticeable around 100 °C, as can be seen from **Fig. 5a and 5b**. Similar observations were made in DMA for other DHPCs and their CB derivatives, on the relative allocation and shifting manner of the three dispersions.

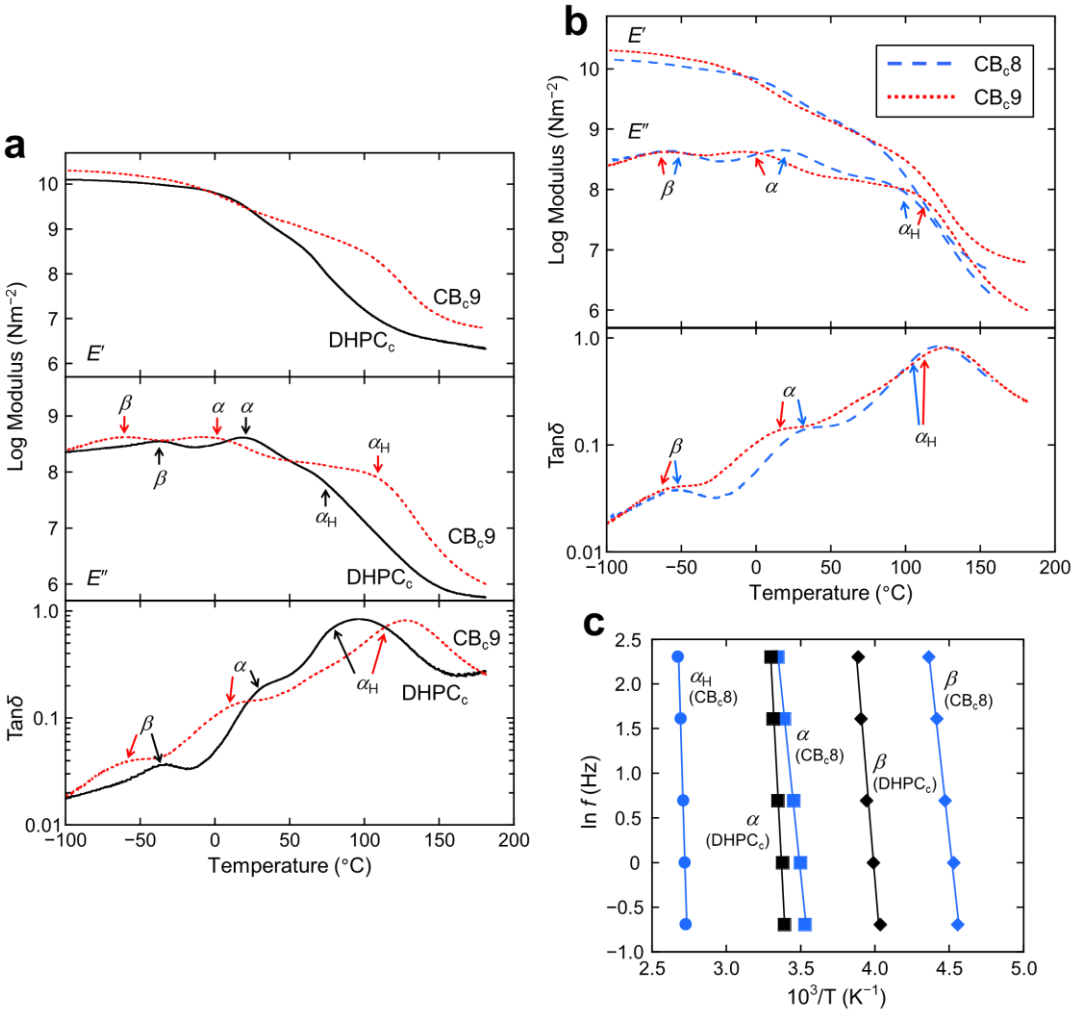

Fig. 5. DMA data: (a) and (b), comparisons of temperature dependence (measured at 1.0 Hz) of the storage modulus (E'), loss modulus (E''), and loss factor (tanδ) for CB_c9 (dotted line in red) with those for $DHPC_c$ (solid line in black in (a)) and CB_c8 (broken line in blue in (b)); (c), illustration of Arrhenius plots of ln f vs. 1000/T for the β and α transitions for CB_c8 and $DHPC_c$ samples. As to the α_H process, the plot was made only for CB_c8 with rough reading of the corresponding E'' peak position.

With reference to the T_g data (from DSC), α here is reasonably taken as the principal dispersion reflecting the micro-Brownian molecular relaxation accompanied by the glass transition of the respective cellulose derivatives. In **Table 3**, readings of

the α relaxation temperature T_α from the corresponding E''-peak position are listed for several samples examined by DMA; definitely, T_α shifts to lower temperatures with increasing % Butyral of CB. The second prominent signal β appearing at temperatures below −30 °C may be assigned to a sub-transition coming from relaxation of the voluminous side-chains of the derivatives. The last α_H signal can be associated with slippage of the trunk chains of DHPC and CB, and therefore the films would undergo plastic flow in the temperature range concerned. However, the entanglement or association between the bulky side-chains should restrain, more or less, the translational movement of the molecules as a whole. This commonly yields a plateau on the E' curves at higher temperatures, as discerned in the modulus data in **Fig. 5a**. The entangling effect is properly more conspicuous in CB samples compared to the case in the starting DHPCs, by virtue of the "necklace-like" ring structure produced in the side chains. In fact, the butyral derivatives were always superior to the DHPC precursors in the magnitude of E' at temperatures above 70 °C. On the other hand, the presence of such a ring structure in the side chains would augment the free volume in the polymer solid, and this augmentation should operate to more readily activate both the local and main chain motions; thereby, the β and α relaxations of CBs can emerge at an earlier stage on heating in comparison with the respective situations of DHPCs.

Further experiments of DMA were carried out on $DHPC_c$, CB_c8, and CB_c9 films with various oscillatory frequencies (f = 0.5, 1, 2, 5 and 10 Hz). As usually expected, the dispersion signals β, α, and α_H shifted to higher temperature positions with an increase of the applied frequency. The relations between the frequency and the respective transition temperatures (from E'' data) were plotted in an Arrhenius fashion, as exemplified in **Fig. 5c**. From the slope of such plots, the apparent activation energy (ΔE_a) required for each thermal transition process can be calculated by the following equation:

$$\Delta E_a = -R\left[\frac{d(\ln f)}{d\left(1/T\right)}\right] \qquad (7)$$

where T is the transition temperature in K, and R is the universal gas constant.

$DHPC_c$ offered data of $\Delta E_a(\beta) \approx 180$ kJ/mol and $\Delta E_a(\alpha) \approx 280$ kJ/mol. The latter

ΔE_a value of the primary α transition may be in a permissible range, in comparison with the corresponding data (160–210 kJ/mol) referring to conventional synthetic homopolymers [19]. However, the $\Delta E_a(\beta)$ data is far beyond the values 40–80 kJ/mol usually observed for secondary transitions of the conventional polymers [19, 20]; this rationalizes that β here is associated with the development of a thicker layer of ether side-chains (% Dhp > 70) around the cellulose backbone. Concerning the butyral derivatives, the following data were assessed; for CB_c8, $\Delta E_a(\beta) \approx 135$ kJ/mol, $\Delta E_a(\alpha) \approx 140$ kJ/mol, and $\Delta E_a(\alpha_H) > 350$ kJ/mol, the last data being estimated with great uncertainty, and for CB_c9, $\Delta E_a(\beta) \approx 130$ kJ/mol and $\Delta E_a(\alpha) \approx 145$ kJ/mol. Thus the introduction of butyral moieties lowered both $\Delta E_a(\beta)$ and $\Delta E_a(\alpha)$ and allowed the heights of the two energy barriers to approach each other. The thermal transition behavior of the CB materials seems to be seriously dominated by the ringed side-chain regions, while the cellulose backbone is present as sustainer in the materials.

Fig. 6 illustrates stress-strain curves obtained for selected films of DHPC and CB in a tensile test at ~23 °C and 50 % r.h. All of the test samples exhibited much better ductility, compared with films of regenerated cellulose and other traditional cellulose derivatives. Particularly DHPC films were highly ductile and showed a large elongation at break (ε_b) exceeding 140 % that increased with an increase in MS_{dhp}; i.e., ε_b = 145 % for $DHPC_c$ of MS_{dhp} = 6.43, ε_b = 196 % for $DHPC_b$ of MS_{dhp} = 8.03, and ε_b = 267 % for $DHPC_a$ of MS_{dhp} = 9.16. After butyralization, the ε_b value of the respective DHPC samples decreased more or less, but their tensile strength (σ_b) was apparently enhanced to improve the tenacity as deformable material. The introduced annular structures would accelerate an effective chain entanglement in the stretching process of the CB films.

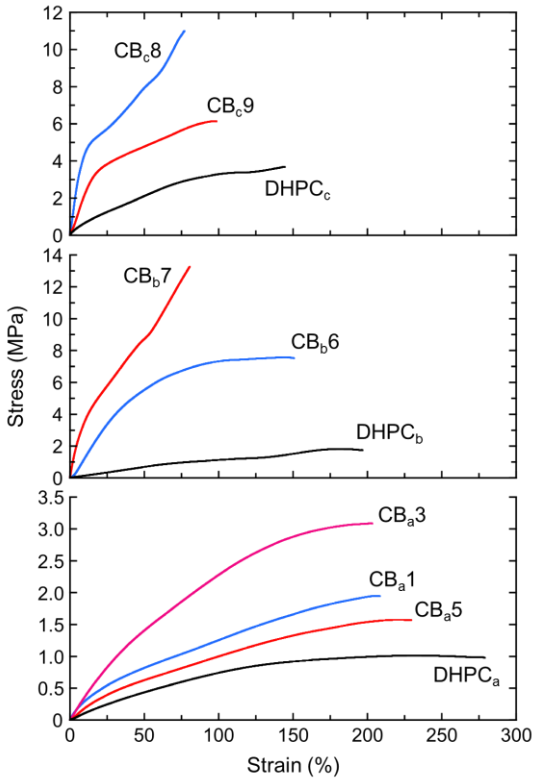

Fig. 6. Stress-strain data for DHPC and CB films at 23 °C and 50 % r.h.

A balanced performance in ductility and tenacity for the objective material may be measured by the toughness which is defined as the integral area under a given stress-strain curve. **Table 3** includes data of the toughness calculated for CB and DHPC films. Definitely, the introduction of ring structures into the side chains of DHPC resulted in an appreciable increase of the film toughness. However, the changing manner did not follow a simple monotonic dependence on % Butyral; for example, the toughness 2.0 MPa of $DHPC_b$ improved to 8.7 MPa of CB_b6 with 3.8 % Butyral, and then dropped to 6.0 MPa of CB_b7 with 7.8 % Butyral despite increasing in σ_b. In samples of higher % Butyral, such as CB_a5 and CB_b7, various sizes of ring structures involving eight and more atoms are formed in the side chains, as evidenced by the data of δ_8/δ_5 = 1.7 (CB_a5) and 1.5 (CB_b7). Such heterogeneity in macro-cyclic structures would give rise to rather irregular chain-entanglements to be a

morphological defect in the CB films on stretching. Additional notice should be attracted to the content of carbohydrate sustainer, i.e., % AGU, in CBs. Confronting the structural data with the tensile results in **Table 3**, we can infer that the content of AGU ≥ 20 % may be required for CB films to exercise a reasonable mechanical performance.

4. Conclusion

In summary, we succeeded in fabrication of high performance films using CB synthesized from native cellulose via DHPC as precursor. The CB products had two forms of annular structures, five-membered ring and eight or more-membered one, on the side chains and were easily molded into a thin film by hot pressing. The CB films were wholly amorphous (T_g < 25 °C), highly transparent, and, conveniently, provided a refractive index slightly lower than that (~1.51) of conventional glass. They were insoluble in water, but showed a good adhesive property to glass plates due to the amphiphilic character. DMA results revealed that the original semi-rigid cellulosic molecule was highly plasticized by a surrounding layer of dihydroxypropyl sequences. The flexible polyether side-chains were primarily responsible to the ductile behavior observed for both DHPC and CB films in the tensile test. The butyral modifier enabled CB films to gain a free volume, but significantly improved the toughness relative to that of DHPC films in the stretching process, by virtue of the more effective chain entangling in which the ring structures were involved. These CB films may be comparable to commercial PVB films in optical and mechanical performances and therefore possess a potential applicability as interlayer for laminated glasses. However, there still remains room for refinements on the optimal chemical composition (% Dhp/Butyral/AGU) of CB to realize much better tensile properties.

Acknowledgments

This work was supported by a Grant-in-Aid for Scientific Research (23-01402) of the JSPS Postdoctoral Fellowship for Foreign Researchers, and Dr. Chang thanks the

National Natural Science Foundation of China (21304021).

Appendix A. Supplementary data

Supplementary data related to this article can be found at http://

References

[1] Jeong HK, Rooney M, David DJ, MacKnight WJ, Karasz FE, Kajiyama T. Polymer 2000; 41 (15): 6003–6013.

[2] Edgar KJ, Buchanan CM, Debenham JS, Rundquist PA, Seiler BD, Shelton MC, Tindall D. Prog Polym Sci 2001; 26 (9): 1605–1688.

[3] Klemm D, Heublein B, Fink HP, Bohn A. Angew Chem Int Ed 2005; 44 (22): 3358–3393.

[4] Nishio Y. Adv Polym Sci 2006; 205: 97–151.

[5] Klemm D, Kramer F, Moritz S, Lindstrim T, Ankerfors M, Gray D, Dorris A. Angew Chem Int Ed 2011; 50 (24): 5438–5466.

[6] Schnepp Z. Angew Chem Int Ed 2013; 52 (4): 1096–1108.

[7] Retegi A, Gabilondo N, Pena C, Zuluag R, Castro C, Ganan P, de la Caba K, Mondragon I. Cellulose 2010; 17 (3): 661–669.

[8] Qi H, Cai J, Zhang L, Kuga S. Biomacromolecules 2009; 10 (6): 1597–1602.

[9] Aulin C, Salazar-Alvarez G, Lindström T. Nanoscale 2012; 4 (20): 6622–6628.

[10] Nishio Y. Hyperfine Composites of Cellulose with Synthetic Polymers. In: Gilbert RD, editor. Cellulosic Polymers, Blends and Composites. Munich: Hanser; 1994. p. 95–113 [chapter 5].

[11] Aoki D, Teramoto Y, Nishio Y. Cellulose 2011; 18 (6): 1441–1454.

[12] Yamanaka H, Teramoto Y, Nishio Y. Macromolecules 2013; 46 (8): 3074–3083.

[13] Imran M, El-Fahmy S, Revol-Junelles AM, Desobry S. Carbohydr Polym 2010; 81 (2): 219–225.

[14] Almasi H, Ghanbarzadeh B, Entezami AA. Int J Biol Macromol 2010; 46 (1): 1–5.

[15] Chang C, Teramoto Y, Nishio Y. J Polym Sci Part A Polym Chem 2013; 51 (17): 3590–3597.

[16] Tezuka Y, Imai K, Oshima M, Chiba T. Polymer 1989; 30 (12): 2288–2291.

[17] Seferis JC. Polymer handbook, Vol. 2 (4th edn.): Wiley, New York, 1999; pp VI/571–582.

[18] Juang YJ, Lee LJ, Koelling KW. Polym Eng Sci 2001; 41 (2): 275–292.

[19] Takayanagi M. Mem Fac Eng Kyushu Univ 1963: 23 (8): 41–96.

[20] Ishida Y, Matsuo M, Ueno Y, Takayanagi M. Kolloid-Z. 1964; 199 (1): 67–68.